Research on interface properties of InGaAs photocathode with nanowire structure

JING GUO[1,*], YUANYUAN LI[2]
[1]*School of Automation, Nanjing Institute of Technology, Nanjing 211167, China*
[2]*NARI Technology Co., Ltd, Nanjing 211106, China*

InGaAs photocathode with nanowire structure is studied by first-principles approach. The nanowire-structured InGaAs photocathodes with GaAs or InP substrate are compared from three aspects: lattice structure, electronic structure and optical properties. Interfaces of $In_{0.5}Ga_{0.5}As$-GaAs and $In_{0.5}Ga_{0.5}As$-InP are focused on research. In order to better describe the optical properties, the light reception on the side of InGaAs nanowires is also analyzed. Crystal structures close to the two sides of interfaces are both relaxed. Electronic structure and optical properties shows that the photocathode with GaAs substrate is more beneficial to the absorption of light in the near-infrared band. In additional the electric field distribution at the interface promote the transition of photoelectrons. Thereby the photoemission efficiency of the photocathode is improved.

1. Introduction

Negative electron affinity (NEA) GaAs photocathodes have been widely used in low-light night vision devices and spin-polarized electron sources due to high quantum efficiency, low dark emission and concentrated emitted electron energy and angle [1-4]. With the development of nanotechnology, III-V semiconductors with nanowire surfaces also have the advantages of high electron mobility and high light absorption rate. They have a wide range of applications in LEDs, lasers, solar cells and photo detection devices [5-9]. Zou Jijun et al. studied the nanowire structure GaAs photocathode, as shown in Fig. 1. The quantum efficiency curve was given [10].
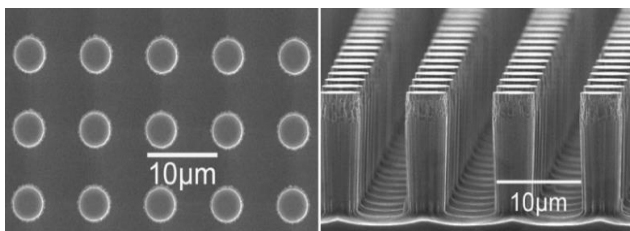

Fig. 1. Nanowire GaAs photocathode structure [10]

In element is added in order to broaden the spectral response range of GaAs in the infrared. The ternary InGaAs photocathode possibly have a better spectral response in the infrared region due to the In addition. This paper attempted to establish GaAs substrate-$In_{0.5}Ga_{0.5}As$

nanowire structure ($In_{0.5}Ga_{0.5}As$-GaAs) and InP substrate-$In_{0.5}Ga_{0.5}As$ nanowire structure ($In_{0.5}Ga_{0.5}As$-InP) photocathode models based on Zou Jijun's research on nanowire GaAs photocathode [10]. The electrical and optical properties of $In_{0.5}Ga_{0.5}As$-GaAs, $In_{0.5}Ga_{0.5}As$-InP interfaces and GaAs, InP surfaces in the nanowire InGaAs photocathode are studied using first-principles research methods.

2. Computational details

The nanowire structure $In_{0.5}Ga_{0.5}As$-GaAs and $In_{0.5}Ga_{0.5}As$-InP models are shown in Fig. 2. The lower right corner of Fig. 2 is the schematic diagram of three-dimensional InGaAs photocathode with nanowire structure. Zinc blende structure $In_{0.5}Ga_{0.5}As$ on InP or GaAs substrate is designed as nanowires. As shown in Fig. 2, the letter D represents the nanowire diameter and P represents the nanowire period. Therefore, according to the schematic diagram of the nanowire photocathode, two interface models $In_{0.5}Ga_{0.5}As$-GaAs and $In_{0.5}Ga_{0.5}As$-InP are established. Then the side and top views are shown in Fig. 2. H atoms are used to saturate dangling bonds to simulate the bulk environment around the interfaces. The top view of the InP substrate and GaAs substrate surfaces are also shown in Fig. 2.

All of the interfaces and surfaces models' calculations are performed by using the Vienna Ab-initio Simulation Package (VASP) [11–14] based on density functional theory (DFT) combined with PW91 general gradient approximation (GGA) exchange correlation functional

[15]. Vanderbilt ultrasoft pseudopotentials supplied by VASP [16] are used to optimize atoms. The calculation of the reconstruction surface models selects 8×4×1 as the number of Monkhorst-Pack [17] k points. The plane wave cut-off energy is 400 eV. The slab is considered fully relaxed when the interatomic forces are all below 0.03 eV/Å. The error in these calculations is estimated to be ± 0.1 eV. All calculations are carried in reciprocal space with Ga: $3d^{10}\,4s^2\,4p^1$, In: $4d^{10}5s^2\,5p^2$, As: $4s^24p^3$ and P: $3s^23p^3$ as the valence electrons.
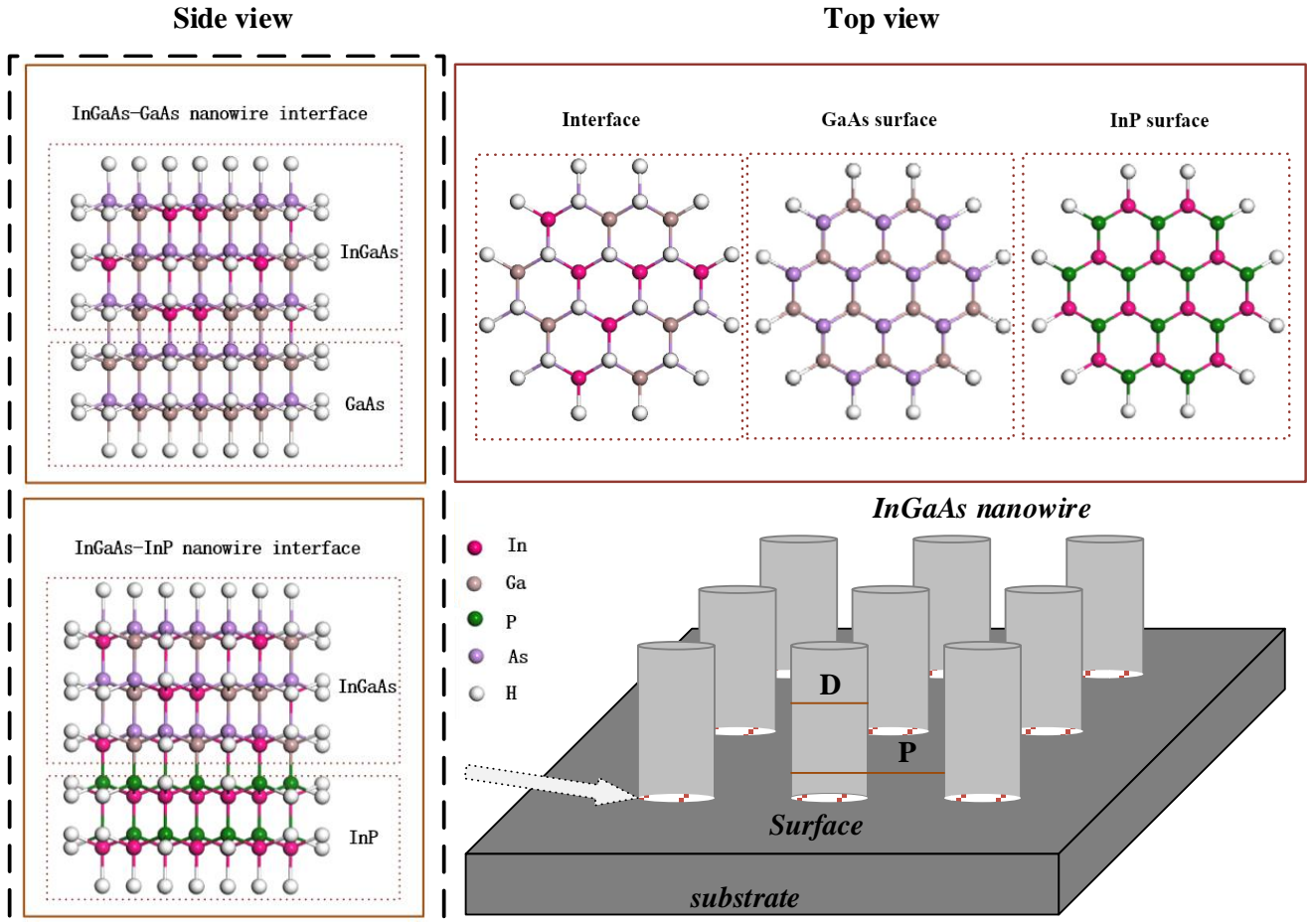

Fig. 2. Interfacial structure of $In_{0.5}Ga_{0.5}As$-GaAs and $In_{0.5}Ga_{0.5}As$-InP nanowires (color online)

3. Results and discussion

3.1. Lattice structure

The lattice constants of $In_{0.5}Ga_{0.5}As$, GaAs and InP are different. Therefore the lattice structures on both sides of the interface of $In_{0.5}Ga_{0.5}As$-GaAs and $In_{0.5}Ga_{0.5}As$-InP have been changed after geometry optimization. The bond length along the Z direction is shown in Fig. 3. Max, Min and Mean represent the maximum, minimum and mean value of the bond length of each layer.
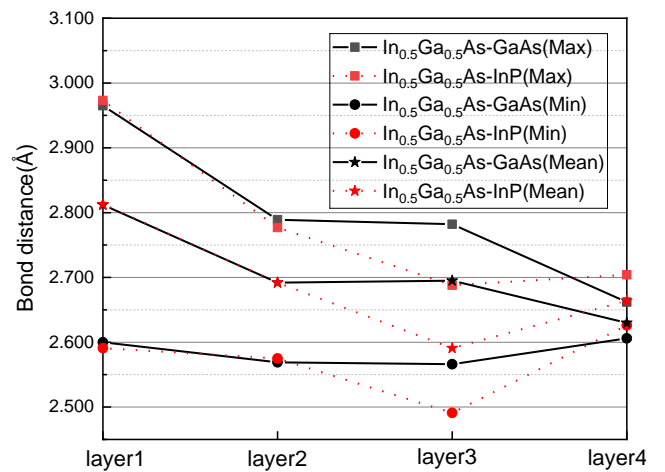

Fig. 3. The bond length along the Z direction on both sides of the interfaces (color online)

In the perfect bulk structure, the Z bond length of GaAs, InP and InAs is 2.498 Å, 2.588 Å and 2.688 Å. Then the bond length in the XY plane of GaAs, InP and InAs is 2.486 Å, 2.757 Å and 2.676 Å respectively. For the $In_{0.5}Ga_{0.5}As$-GaAs interface, the first and second layers are $In_{0.5}Ga_{0.5}As$ structures and the third and fourth layers are GaAs structures. Their average bond lengths have increased after optimization, as shown in Fig. 3. Similarly, for the $In_{0.5}Ga_{0.5}As$- InP interface, the first and second layers are $In_{0.5}Ga_{0.5}As$ structure and the third and fourth layers are InP structure. It is found that the average bond length has also increased. It means that the $In_{0.5}Ga_{0.5}As$-GaAs and the $In_{0.5}Ga_{0.5}As$-InP interfaces both have atom relaxation along the Z direction.

The bond lengths of the first and fourth layers in the XY plane are shown in Table 1. In the XY plane, the increase in bond length is more obvious. The average bond lengths of the $In_{0.5}Ga_{0.5}As$ (the first layer) is 2.831 Å and 2.835 Å and those of the underlying GaAs and InP (the forth layer) are 2.861 Å and 2.839 Å while those of the pure GaAs and InP surface after optimization in the XY plane are 2.485 Å and 2.690 Å, respectively.

Table 1. The bond lengths of the $In_{0.5}Ga_{0.5}As$-GaAs and $In_{0.5}Ga_{0.5}As$-InP interfaces (Å)

		$In_{0.5}Ga_{0.5}As$-GaAs	$In_{0.5}Ga_{0.5}As$-InP
	Interfaces		
First layer	Maximum	3.109	3.150
	Minimum	2.555	2.556
	Average	2.831	2.835
Fouth layer	Maximum	3.310	3.095
	Minimum	2.590	2.718
	Average	2.861	2.839

It is proved that the interface is relaxed along the Z direction and in the XY plane when the nanowire $In_{0.5}Ga_{0.5}As$ structure is grown on the GaAs or InP substrate. But the GaAs or InP surface without the growth of $In_{0.5}Ga_{0.5}As$ nanowire area is compressed.

3.2. Electronic structure of interfaces

According to the band gap formula: $E_g = 0.4x^2 - 1.50x + 1.432$ [18], where x is the In composition. When x=0.5, the theoretical and the calculated band gap of classical bulk $In_{0.53}Ga_{0.47}As$ is 0.732eV and 0.574 eV [19] and that of $In_{0.53}Ga_{0.47}As(100)\beta_2(2\times4)$ surface is 0.087 eV [19]. The calculated band gaps of the $In_{0.5}Ga_{0.5}As$-GaAs and $In_{0.5}Ga_{0.5}As$-InP interfaces with nanowire structures are 0.046 eV and 0.054 eV respectively while those of pure GaAs and InP substrate surfaces are 0.086 eV and 0.010 eV. Therefore, the band gap of $In_{0.5}Ga_{0.5}As$-GaAs

and $In_{0.5}Ga_{0.5}As$-InP are reduced as the analysis above. It is much easier for photoelectrons transition to the conduction band in the interface than in pure GaAs and InP substrates. For nanowire-structured photocathodes, the photoelectrons escape is closely related to the surface work function. The work functions of $In_{0.5}Ga_{0.5}As$-GaAs and $In_{0.5}Ga_{0.5}As$-InP are 4.967 eV and 5.2 eV respectively while those for GaAs and InP substrate surfaces are 5.029 and 5.276 eV. The work functions of the interfaces are also slightly lower than that of the pure surface. It means that the interfaces are also a favorable factor for the photoelectrons' escape.

The energy band and surface work function of the photocathode should also be analyzed combining with electron migration. Charge transfer coefficient c [20] is shown as Eq. (1)

$$c = \frac{1}{N}\sum_{Q=1}^{N}\frac{\vartheta(\Omega)}{OS(\Omega)} = \langle\frac{\vartheta(\Omega)}{OS(\Omega)}\rangle \qquad (1)$$
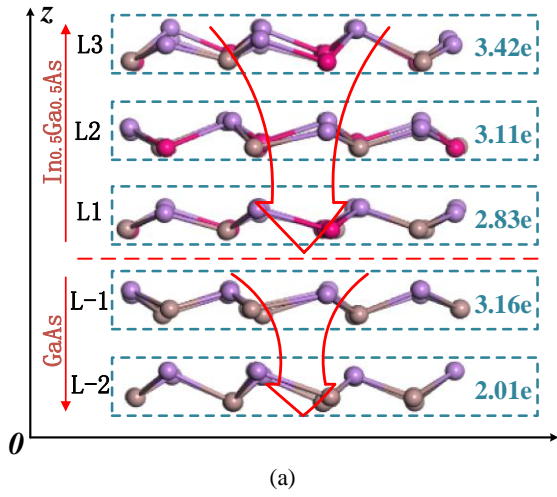
where N is the total number of atoms in the system, $\vartheta(\Omega)$ is the topological charge number, and $OS(\Omega)$ is the nominal oxidation state. The charge transfer coefficient indicates the strength of interfacial ionization, which provides a better measure for the interfacial bond formation. The calculated charge transfer coefficients of $In_{0.5}Ga_{0.5}As$-GaAs and $In_{0.5}Ga_{0.5}As$-InP at the interface are 0.496 and 0.403, both between 0.3 and 0.6, which is consistent with ionization coefficients of group III-V compounds in the Ref. [20]. InGaAs photocathode with InP substrate has smaller ionization coefficient value and stronger ionization while that with GaAs substrate has weaker ionization.

Table 2 shows the charge transfer of each layer in the $In_{0.5}Ga_{0.5}As$-GaAs and $In_{0.5}Ga_{0.5}As$-InP interfaces. The meanings of L-2, L-1, L1, L2, and L3 in Table 2 are shown in Fig. 4.

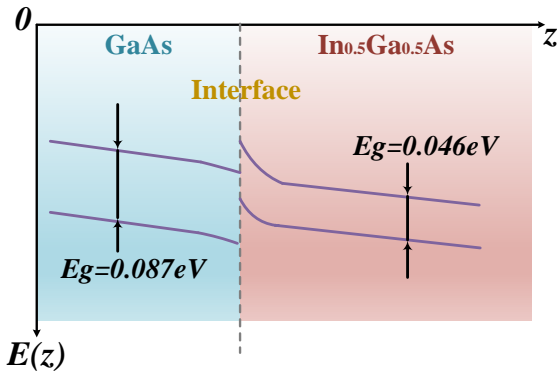*Table 2. Transfer charge of each layer in the $In_{0.5}Ga_{0.5}As$-GaAs and $In_{0.5}Ga_{0.5}As$-InP interfaces*

layer	L-2	L-1	L1	L2	L3
$In_{0.5}Ga_{0.5}As$-GaAs (e)	2.01	3.16	2.83	3.11	3.42
$In_{0.5}Ga_{0.5}As$-InP (e)	5.85	7.09	4.63	3.24	3.61

In Table 2, the numbers of lost electrons at L-2, L-1, L1, L2 and L3 in the $In_{0.5}Ga_{0.5}As$-GaAs interface are 2.01, 3.16, 2.83, 3.11 and 3.42, respectively. The nanowire $In_{0.5}Ga_{0.5}As$ generated a built-in electric field directing from inside to the interface and the GaAs substrate formed a built-in electric field directing from the interface to the inside of substrate (as shown in Fig. 4(a)). But the interface has a potential barrier, just as a certain obstacle for the transition of electrons from the substrate to InGaAs. Fig. 4(b) shows the band structure near the interface.
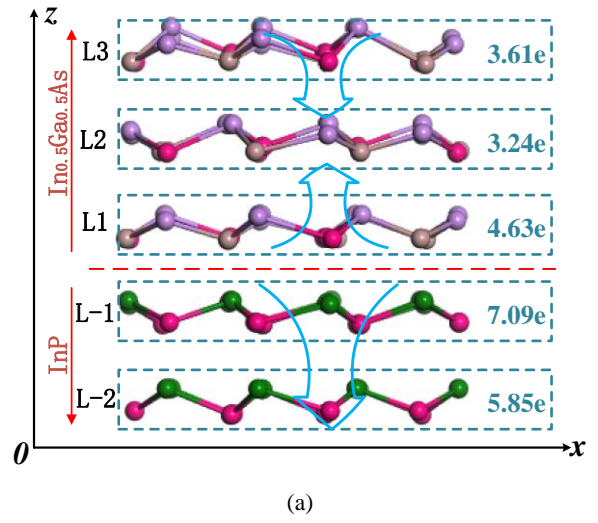
(a)

(b)

Fig. 4. Electronic structure of the $In_{0.5}Ga_{0.5}As$-GaAs interface (a) Gain and loss of electrons of each layers in $In_{0.5}Ga_{0.5}As$-GaAs interface (b) Energy band structure of $In_{0.5}Ga_{0.5}As$-GaAs (color online)

According to Gauss's theorem, the electric field intensity between layers is as shown in Eq. (2).
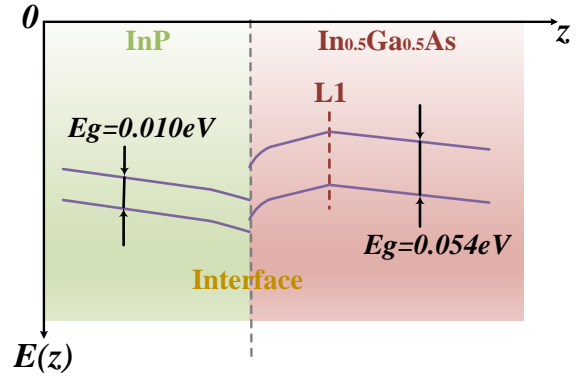
$$E = \frac{Q}{\varepsilon S} \qquad (2)$$

where E is the electric field intensity, Q is the interlayer charge, ε is the static permittivity, according to the formula $\varepsilon=0.67x^2+1.53x+12.9$ [21] (x is the In component), when x=0.5, ε is 13.9, S is the layer's area. According to Eq. (2), the electric field intensities on both sides of the interface are 0.431 and 0.836 mV/m, respectively. The generated built-in electric field is directed from $In_{0.5}Ga_{0.5}As$ to GaAs which prevents the photoelectrons generated by the emission layer entering the GaAs substrate while the photoelectrons generated by the GaAs substrate have the opportunity to enter the $In_{0.5}Ga_{0.5}As$ emission layer.

Compared with the interface with GaAs substrate, the loss of electrons in the $In_{0.5}Ga_{0.5}As$-InP interface is slightly different, as shown in Fig. 5.

(a)

(b)

Fig. 5. Electronic structure of the $In_{0.5}Ga_{0.5}As$-InP interface (a) Gain and loss of electrons of each layers in $In_{0.5}Ga_{0.5}As$-InP interface (b) Energy band structure $In_{0.5}Ga_{0.5}As$-InP (color online)

In Fig. 4, GaAs loses more electrons near the interface and a built-in electric field pointing to the GaAs substrate is formed. In Fig. 5, the InP substrate in which electric field is also built is similar to GaAs in Fig. 4. But the number of electrons lost in the InP substrate is relatively large, which is consistent with the conclusion of the charge transfer coefficient above. It is indicated that the ionicity of the InP substrate is higher than that of GaAs. The potential barrier in the interface is a bidirectional barrier. From the gain and loss of electrons, the potential barrier of the $In_{0.5}Ga_{0.5}As$-InP is significantly higher than that of the $In_{0.5}Ga_{0.5}As$-GaAs. The electric field intensities on both sides of the interface are 0.350 and 1.216 mV/m, respectively. The electric field intensity in the InP substrate is significantly higher than the GaAs substrate. The energy band structure of $In_{0.5}Ga_{0.5}As$-InP is as shown in Fig. 5(b). The photoelectrons transition from the substrate to the emission layer is much more difficult than $In_{0.5}Ga_{0.5}As$-GaAs.

3.3. Optical properties of the interfaces

The photoelectron emission of the InGaAs photocathode is shown in Fig. 6 combined with the interface structures shown in Fig. 2. The photocathode surface is a nanowire array. The light collection on the InGaAs photocathode is divided into the following four cases according to the light incident angle θ.
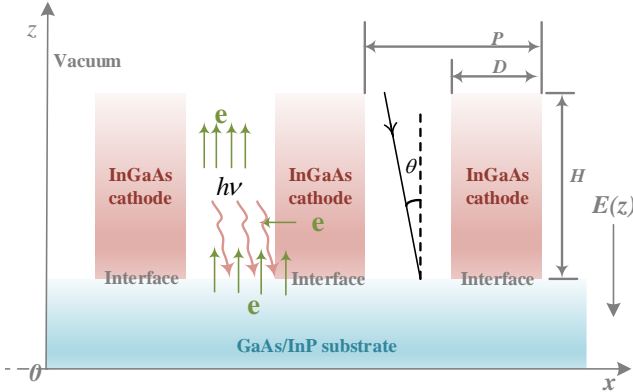

Fig. 6. Optical absorption and photoelectron emission of interface and surface (color online)

I) $\theta = 0°$

Photons are only collected (absorption and reflection) on the top surface of the InGaAs emission layer and the surface of the GaAs or InP substrate. The coefficient β is defined as the ratio of the optical signal collected on the top surface of the nanowire photocathode to the surface of the substrate and its value is approximated to $\beta = \frac{D^2}{P^2 - D^2}$ according to the derivation of plane geometry, where D is the diameter of the nanowire and P is the period of the nanowire, as shown in Fig. 6.

II) $0° < |\theta| < \tan^{-1}(\frac{P-D}{H})$

Photons are collected by three surfaces: the first is the surface of the GaAs or InP substrate, the second is the side surface of the $In_{0.5}Ga_{0.5}As$ nanowire emission layer, which is completely light-receiving and the third is the top surface of the $In_{0.5}Ga_{0.5}As$ nanowire.

III) $|\theta| = \tan^{-1}(\frac{P-D}{H})$

The top and one side of the $In_{0.5}Ga_{0.5}As$ nanowire is completely illuminated while the GaAs or InP substrate surface no longer receive light.

IV) $\tan^{-1}(\frac{P-D}{H}) < |\theta| < 90°$

One side surface of the $In_{0.5}Ga_{0.5}As$ nanowire is partially light-receiving. The area depends on the incident angle θ of the light. The top surface is completely light-receiving. The GaAs or InP substrate surface is not exposed to light.

The quantum efficiency of traditional reflective photocathode, which is shown in Eq. (3), is related to the absorption and reflection of the photocathode surface [22].

$$Y_R(h\upsilon) = \frac{P(1-R)}{1 + \frac{1}{\alpha L}} \tag{3}$$

where P is the electron escape probability, R is the reflectivity of the photocathode, L is the electron diffusion length, and α is the absorption coefficient. P and R are both related to InGaAs surface parameters [19]. If the emission layer is thin, L is closely related to the interface properties [23]. The reflectivity R and the absorption coefficient α are functions of the incident photon energy, which characterize the strength of the electron's ability to absorb photons. It is not only related to the interface and surface properties, but also to the specific structure of the photocathode.

For the four cases of InGaAs photocathode with nanowire structure, the photoemission near the interface is related to the optical and photoelectric properties of the substrate (GaAs or InP) surface, the interface ($In_{0.5}Ga_{0.5}As$-GaAs or $In_{0.5}Ga_{0.5}As$-InP), and the side surface of the nanowire $In_{0.5}Ga_{0.5}As$ emission layer. The optical absorption coefficients of these five surfaces are shown in Fig. 7.
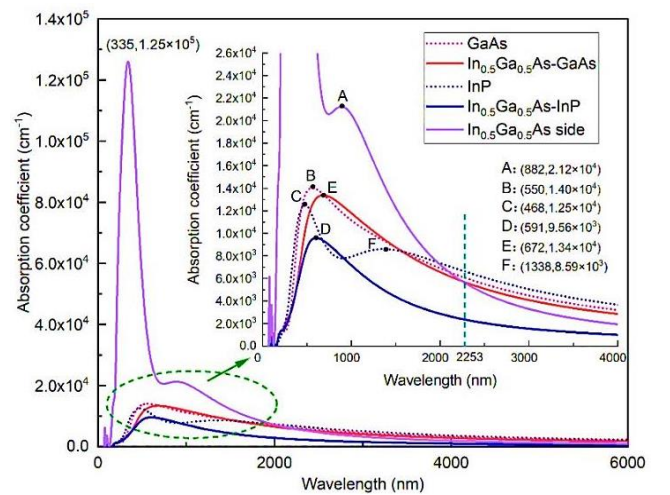

Fig. 7. Optical absorption coefficients of GaAs surface, InP surface, $In_{0.5}Ga_{0.5}As$-GaAs interface, $In_{0.5}Ga_{0.5}As$-InP interface and $In_{0.5}Ga_{0.5}As$ side surface (color online)

The absorption coefficient of the $In_{0.5}Ga_{0.5}As$ side surface has an obvious peak (1.25×10^5 cm^{-1}) at 335 nm, followed by a secondary peak (2.12×10^4 cm^{-1}) at 882 nm (point A in Fig. 7). The absorption peaks of the GaAs substrate, the $In_{0.5}Ga_{0.5}As$-GaAs interface and the $In_{0.5}Ga_{0.5}As$-InP interface are at point B (550 nm, 1.40×10^4 cm^{-1}), point E(672 nm, 1.34×10^4 cm^{-1}) and point D (591 nm, 9.56×10^3 cm^{-1}). The InP substrate has two absorption peaks which are at point C (468 nm, 1.25×10^4 cm^{-1}) and point F (1338 nm, 8.59×10^3 cm^{-1}).

Since the target response of the InGaAs photocathode is the near-infrared band, the absorption peak at 335 nm is not discussed in detail. The absorption coefficient of the $In_{0.5}Ga_{0.5}As$ side surface at 882 nm is much bigger than those of the substrates and the interfaces. The $In_{0.5}Ga_{0.5}As$-InP interface has the minimum absorption coefficient. When the wavelength is greater than 2253 nm, the absorption coefficient of the nanowire $In_{0.5}Ga_{0.5}As$ side surface is only higher than that of the $In_{0.5}Ga_{0.5}As$-InP interface, and lower than the other three surfaces or interfaces. Fig. 8 shows the reflectivity of each relevant surface and interface of the InGaAs photocathode with nanowire structure.
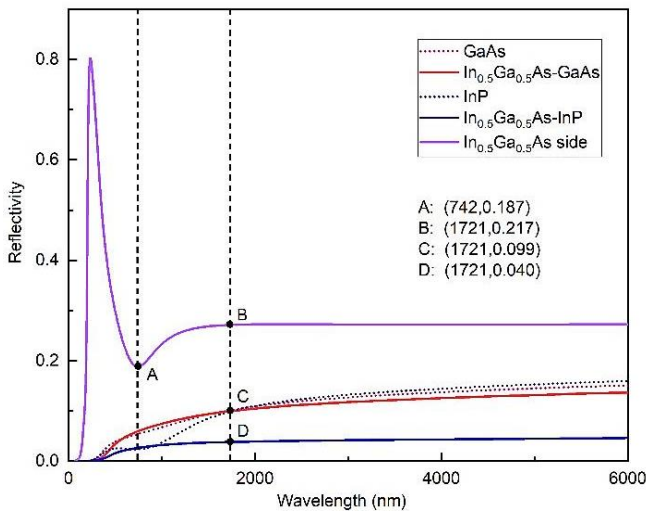

Fig. 8. Reflectivity of GaAs surface, InP surface, $In_{0.5}Ga_{0.5}As$-GaAs interface, $In_{0.5}Ga_{0.5}As$-InP interface and $In_{0.5}Ga_{0.5}As$ side surface (color online)

From Fig. 8, the reflectivity of the InGaAs side surface is the purple solid line. It can be clearly seen that there is a reflection peak in the short waveband. Like the absorption coefficient, the short waveband is not the main response waveband of the InGaAs photocathode and is not discussed in detail. The point A at 742 nm is the position with the lowest reflectivity (0.187) of the $In_{0.5}Ga_{0.5}As$ side surface. Then the reflectivity gradually increases and tends to stabilize at point B (0.217, 1721 nm). However it is still much higher than those of the $In_{0.5}Ga_{0.5}As$-GaAs interface, InP or GaAs substrate surface at point C (0.099). The reflectivity of the $In_{0.5}Ga_{0.5}As$-InP interface is the lowest,

which is almost maintained at 0.040 in the target near-infrared band.

Zou Jijun et al. pointed out that the GaAs nanowire structure photocathode had the parameters as D=3 or 6 μm, P=6 or 10 μm and H=8.5 or 14.46 μm in Ref. [10]. The actual parameters of InGaAs nanowire structure photocathode has not been given in any reference before. Therefore a set of GaAs data (D=3 μm, P=6 μm, H=8.5 μm) in Ref. [10] is substituted into the calculated θ angle in InGaAs photocathode here.

I) When $\theta = 0°$, the ratio of the optical signal collected on the top of InGaAs surface and the substrate surface is $\beta = 1/3$, that is, 75% of the light is absorbed by the substrate surface when the light is irradiated vertically. In Fig. 7, the optical absorption coefficient of GaAs substrate is larger than that of InP substrate in the range of 468-1557 nm while that of InP is slightly larger than GaAs when the wavelength is greater than 1557 nm. The reflectivity of GaAs is higher than InP when the wavelength is less than 1721 nm and that of InP is greater than GaAs when the wavelength is greater than 1721 nm, as shown in Fig. 8. The GaAs is more favorable than InP used as the substrate of the InGaAs photocathode with nanowire structure in the range from 1557 to 1721 nm considering the absorption and reflection at the interface.

II) When 0°<|θ|<19.44°, the light is irradiated to three sides: part of the substrate surface, the interface and the $In_{0.5}Ga_{0.5}As$ side surface (full light receiving). At this time, the light absorption is mainly absorbed by the $In_{0.5}Ga_{0.5}As$ side surface which has the biggest absorption coefficient when the wavelength is less than 1721 nm. The absorption coefficient of the $In_{0.5}Ga_{0.5}As$-GaAs interface is similar to that of the GaAs substrate surface and is better than that of the $In_{0.5}Ga_{0.5}As$-InP interface. Meanwhile the reflectivity is also high. So it should be processed on the side of the $In_{0.5}Ga_{0.5}As$ nanowire to reduce the light reflectivity. The performance of the nanowire InGaAs photocathode with GaAs substrate is better than that with InP substrate.

III) When |θ|=19.44°, at this time, the light irradiates the interface and the side surface of $In_{0.5}Ga_{0.5}As$ nanowire, which is basically similar to the second case. The performance of InGaAs photocathode with GaAs substrate is better than that with InP substrate.

IV) When 19.44°<|θ|<90°, just only the side surface of the $In_{0.5}Ga_{0.5}As$ nanowire receives light partly. The properties of the substrate surface and interface do not affect the absorption of light.

In conclusion, from the perspective of optical properties, the nanowire InGaAs photocathode with GaAs substrate is better than that with InP substrate in the target near-infrared band of less than 2 microns. However, the actually photocathode surface still needs to be cleaned and

adsorbed. The optical properties need to be further expanded [24].

4. Conclusions

The nanowire InGaAs photocathode with GaAs substrate or InP substrate are comparatively discussed. The photoemission performance of the photocathode is studied from three aspects: lattice structure, electronic structure and optical properties. From the lattice structure, when the nanowire InGaAs structure grows on the GaAs or InP substrate, the interface is relaxed both in the Z-axis direction and in the XY plane while the surface area of the GaAs or InP without the nanowire growth part is compressed. Considering the electronic structure of the interface, the existence of the interface is conducive to the transition of photoelectrons. Part of the internal photoelectrons in the nanowire InGaAs is provided by the substrate. The $In_{0.5}Ga_{0.5}As$-GaAs interface is more favorable for the transition of photoelectrons than the $In_{0.5}Ga_{0.5}As$-InP interface from the points of the electrons distribution and electric field near the interface. Finally, the optical properties near the interface are analyzed. The nanowire InGaAs photocathode with GaAs substrate has better response than that with InP substrate in the target near-infrared band less than 2 microns. To sum up, the InGaAs nanowire photocathode should be preferentially grown on the GaAs substrate which is conducive to the generation and emission of photoelectrons. Moreover, from the analysis above, part of the photocurrent of the nanowire InGaAs photocathode is contributed by the substrate. The spectral response range and the magnitude of the photocurrent should be considered together with the substrate and the nanowire photocathode.

References

[1] H.-J. Drouhin, C. Hermann, G. Lampel, Phys. Rev. B **31**, 3859 (1985).

[2] G. Vergara, L. J. Gómez, J. Capmany, M. T. Montojo, Vacuum **48**, 155 (1997).

[3] J. P. Estrera, E. J. Bender, A. Giordana, J. W. Glesener, M. Iosue, P. P. Lin, T. W. Sinor, Proc. SPIE **4128**, 46 (2004).

[4] Z. Liu, Y. Sun, S. Peterson, P. Pianetta, Appl. Phys. Lett. **92**, 241107 (2008).

[5] K. Tomioka, J. Motohisa, S. Hara, K. Hiruma, T. Fukui, Nano Lett. **10**(5), 1639 (2010).

[6] I. Aberg, G. Vescovi, D. Asoli, U. Naseem, J. Gilboy, C. Sundvall, A. Dahlgren, K. Svensson, N. Anttu, M. Björk, L. Samuelson, IEEE J. Photovolt. **6**(1), 185 (2015).

[7] W. Hao, Appl. Phys. Lett. **103**(9), 1209 (2013).

[8] J. Zou, W. Zhao, X. Ding, Z. Zhu, W. Deng, W. Wang, Appl. Phys. A **122**(12), 1003 (2016).

[9] L. Liu, Y. Diao, S. Xia, J. Mater. Sci. **54**, 5605 (2019).

[10] J. Zou, X. Ge, Y. Zhang, W. Deng, Z. Zhu, W. Wang, X. Peng, Z. Chen, B. Chang, Optics Express **24**(5), 4633 (2016).

[11] G. Kresse, VASP, Technische University, Wien, 1993.

[12] G. Kresse, J. Furthmüller, Comput. Mater. Sci. **6**, 15 (1996).

[13] G. Kresse, J. Furthmüller, Phys. Rev. B **54**, 11169 (1996).

[14] G. Kresse, J. Hafner, Phys. Rev. B **47**, 558 (1993).

[15] J. P. Perdew, K. Burke, M. Ernzerhof, Phys. Rev. Lett. **77**, 3865 (1996).

[16] G. Kresse, J. Hafner, J. Phys.: Condens. Matter. **6**, 8245 (1994).

[17] H. J. Monkhorst, J. D. Pack, Phys. Rev. B **13**, 5188 (1976).

[18] K. Shim, Thin Solid Films **516**, 3143 (2008).

[19] J. Guo, B. Chang, M. Jin, M. Yang, H. Wang, M. Wang, J. Huang, L. Zhou, Y. Zhang, Appl. Surf. Sci. **288**, 238 (2014).

[20] P. Mori-Sánchez, A. M. Pendás, V. Luaña, J. Am. Chem. Soc. **124**, 14721 (2002).

[21] K. H. Goetz, D. Bimberg, H. Jürgensen, J. Selders, A. V. Solomonov, G. F. Glinskii, M. Razeghi, J. Appl. Phys. **54**, 4543 (1983).

[22] G. A. Antypas, L. W. James, J. J. Uebbing, J. Appl. Phys. **41**, 2888 (1970).

[23] A. W. Walkera, M. W. Denhoff, Appl. Phys. Lett. **111**, 162107 (2017).

[24] X. Yu, Z. Jin, G. Shao, J. Mater. Sci.: Mater. Electron. **33**, 23351 (2022).

*Corresponding author: zdhxgj@njit.edu.cn